Growth Behavior of Pulsed-Laser-Deposited PLZTO Thin Films

Tzu-Feng Tseng and Kuo-Shung Liu
Dept. of Material Science & Engineering, National Tsing-Hua University, Hsinchu 300, Taiwan, R.O.C.

I-Nan Lin
Material Science Center, National Tsing-Hua University, Hsinchu 300, Taiwan, R.O.C.

Jyh-Ping Wang and Yong-Chien Ling
Dept. of Chemistry, National Tsing-Hua University, Hsinchu 300, Taiwan, R.O.C.

Elemental depth profile examined using secondary-ion mass spectroscopy and structural profile examined using grazing-incident X-ray diffractometry were applied to analyze the growth behavior of $Pb_{1-x}La_x(Zr_yTi_{1-y})O_3$ (PLZTO) and $Pb_{1-x}La_xTiO_3$ (PLTO) thin films deposited on a Si substrate. When deposited under a suitably high substrate temperature, the chamber's oxygen pressure was observed to substantially influence the structure of the films. Low oxygen pressures ($P_{O_2} < 0.01$ mbar) deteriorate crystal structure without altering the composition of the films. Deposition of a buffer layer enhanced the formation kinetics of PLZTO and PLTO films. However, sufficiently thick $SrTiO_3$ (~ 500 nm) layer was required to achieve this effect. Using $(La_{0.5}Sr_{0.5})CoO_3/Pt$ materials as double-layer electrodes not only prevented the film-to-substrate interaction, but resulted in preferentially oriented thin films. Ferroelectric properties of the films were thus greatly improved, with remanent polarization (Pr) around 14 ~ 16 $\mu C/cm^2$, coercive force (Ec) around 50 ~ 60 kV/cm, and relative dielectric constant (ϵ_r) around 900 ~ 1,000.

Introduction

Ferroelectric thin films, such as $PbTiO_3$, $Pb(Zr_xTi_{1-x})O_3$, $(Pb_{1-x}La_x)TiO_3$, and $Pb_{1-x}La_x(Zr_yTi_{1-y})O_3$, are promising materials for applications as pyroelectric detectors, nonvolatile memories, and random-access memories (Gnadinger and Bondurant, 1989; Scott and Araujo, 1989; Sheppard, 1992), and thus have been extensively investigated. The pulsed-laser-deposition (PLD) technique has several advantages in synthesizing oxide thin films, such as high deposition rate, flexibility in the requirement for depositing environment, and feasibility in compositional control, and have therefore found extensive use in synthesizing these films (Otsubo et al., 1990; Horwitz et al., 1991; Kidoh et al., 1991; Grabowski et al., 1991; Leuchtner et al., 1992).

The deposition of Pb-containing ferroelectric thin films on Si substrates is, however, rather difficult. The occurrence of a pyrochlore phase is inevitable when the films are grown directly on Si substrate. $SrTiO_3$ buffer layers on Si substrate have been reported as being able to suppress the Pb loss during the process (Yeh et al., 1994, 1995). It can circumvent the cumbersome and uncontrollable approaches such as the addition of excess PbO or postannealing of the low-temperature-deposited films (Roy et al., 1991). However, the growth of Pb-containing ferroelectric films still requires high oxygen deposition pressure to grow pure perovskite phase. No crystalline phase was observed in films deposited at low oxygen pressure ($P_{O_2} < 0.01$ mbar).

In an effort to provide a better understanding of this phenomenon, secondary-ion mass spectroscopy (SIMS) and grazing-incident X-ray diffraction (GIXD) were used to systematically characterize the elemental and structural depth profile of these multilayer thin films. The possible interaction between thin films and substrate is discussed below.

Experimental Studies

The laser beam from a XeCl laser (308 nm, Lambda Physik 205i) with an energy density of 3 J/cm^2 was used for growing $Pb_{1-x}La_x(Zr_yTi_{1-y})O_3$, with $x = 0.05$, $y = 0$ (PLTO)

or $y = 0.3$ (PLZTO), or buffer-layer (i.e., $SrTiO_3$ or $(La_{0.5}Sr_{0.5})CoO_3$) films by a pulsed-laser-deposition technique. The targets of the nominal composition were prepared by the conventional mixed-oxide method. The buffer layers were deposited at 600°C ($P_{O_2} = 1$ mbar), and the PLZTO (PLTO) films were deposited at 500°C or 600°C $P_{O_2} = 1$ mbar). The structure of the films was examined using conventional (θ–2θ) X-ray diffraction (Rigaku, D/max IIB) or the GIXD technique (MAC, MXP-18). The elemental depth profile of the films was examined using SIMS technique (Cameca, IMS-4f). The sputtering rate in SIMS analysis is separately calibrated and is around 0.25 nm/s.

Results and Discussions

Growth behavior

Based on earlier studies (Yeh et al., 1994, 1995), it was assumed that the PLZTO perovskite phase was formed by a two-step process, that is (1) the adhesion of the species contained in the plume onto the substrate as clusters, followed by (2) the transformation of these clusters into a crystalline structure. The source that resulted in Pb-deficiency in the films was assumed to come from the reevaporation of Pb species from the adhered clusters. Using $SrTiO_3$ (STO) as a buffer layer can effectively suppress the Pb loss. The mechanism is presumably an increase in the phase-transformation kinetics. The clusters that adhered onto the STO surface transformed rapidly into the perovskite phase, so that the revaporization rate would be lowered markedly. The (110) textured PLZTO films, which possess an effective dielectric constant around $\epsilon_r = 490$, at 100 kHz, and charge storage density around $Q_C = 1.5\ \mu C/cm^2$, at 50 kV/cm applied field strength, were successfully synthesized.

The Zr^{4+} ions contained in the PLZTO films were observed to be the species that hinders the kinetics of the formation of the perovskite phase. The films that are less susceptible to loss of the Pb^{2+} ions and that perform better can be synthesized by removing Zr ions from PLZTO materials (i.e., PLTO films). The films deposited *in situ* at 450°C ($P_{O_2} = 1$ mbar) for 10 min on platinum-coated silicon, followed by rapidly quenching right after deposition, possessed good dielectric properties, that is, $\epsilon_r = 1346$ and $\tan\ \delta = 0.071$ at 10 kHz ($\epsilon_r = 1297$ and $\tan\ \delta = 0.096$ at 100 kHz) and charge storage density, that is, $Q_C = 5.4\ \mu C/cm^2$ at 50 kV/cm.

The effect of interdiffusion on the phases, the structural depth profiles, and the elemental depth profile in PLTO and PLZTO thin films was examined further using SIMS. Figures 1a and 1b show that interaction between the film and substrate is more significant in PLTO thin films, which is implied by a hump with larger Si-ion counts of Si profile in Figure 1a, whereas the Pb loss is more serious in PLZTO thin films, which is inferred from a significantly lower Pb-to-Si ion count ratio at the surface of PLZTO films (cf. Figure 1b). These results indicate that marked film-to-substrate interaction does not necessarily lead to more serious Pb revaporization at the film's surface. The assumption that the slow-crystalline kinetics of PLZTO films is the cause of high susceptibility in Pb loss is clearly implied.

In addition, Figure 2a shows the X-ray diffraction (XRD) patterns of PLTO films ($\sim$ 800 nm) deposited from the target of the composition $Pb_{0.95}La_{0.05}TiO_3$ under 500°C (1 mbar)

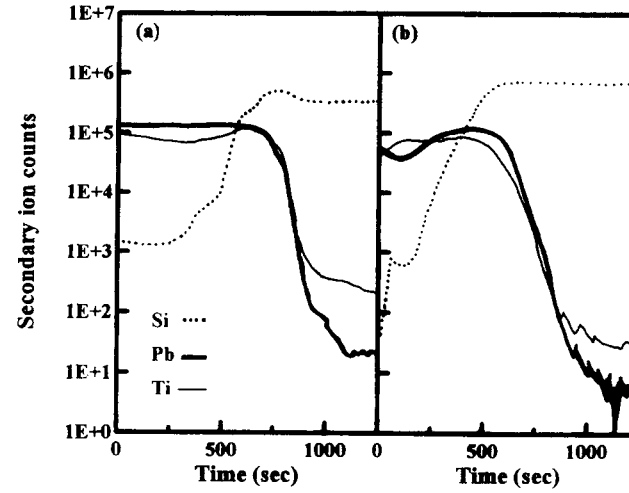

Figure 1. SIMS profiles of (a) PLTO/Si and (b) PLZTO/Si thin films [PLTO:$Pb_{0.95}La_{0.05}TiO_3$; PLZTO: $Pb_{0.95}La_{0.05}(Zr_{0.3}Ti_{0.7})O_3$].

on Pt-coated and uncoated Si substrate, respectively, using $SrTiO_3$ (STO) as a buffer layer. These figures indicated that the STO layer has successfully enhanced the formation of PLTO perovskite on both substrates. STO layers also markedly increased the stability of the PLTO films. Pb loss due to revaporization from the film's surface was not induced, even when the substrate temperature was increased to 600°C ($P_{O_2} < 1$ mbar) or the oxygen pressure was reduced to 0.1 mbar (at 500°C). It should be noted that (a) TiO_2 secondary phase of the rutile structure was observed only in PLTO/STO/Pt/Si and PLTO/Pt/Si films, but not in PLTO/STO/Si and PLTO/Si films. However, Figure 2b indicates that, for PLTO/STO/Si thin films, a noisy background corresponding to the noncrystalline phase was observed when the oxygen pressure used was lower than 0.01 mbar. In the extreme case—$P_{O_2} = 1 \times 10^{-4}$ mbar—most of the diffraction peaks disappear, leaving behind barely perceptible (110) PLTO diffraction peaks. The sources that induced the amorphorization of the films are discussed further later on.

On the other hand, SIMS profiles indicate that the Si species diffuse all the way through the "thin" STO layer, which is pulsed-laser deposited only for 1 min (Figure 3b), whereas the Si ion counts drop markedly for "thick" STO layer, which is pulsed-laser deposited for 15 min (Figure 3a). In other words, sufficiently "thick" STO layers were required to suppress the film-to-substrate interactions. As shown in Figure 4, it is proposed that the STO was formed by the island growth process. When the STO films are "thin," individual STO grains were scattered on the substrates such that a large proportion of the Si surface was still not covered by STO films. The subsequently grown PLZTO (PLTO) will thus interact with the Si materials and induce a large amount of Pb-deficient phase. The intermediate layers are thick and consist of Si, PLZTO (PLTO), and STO phases. Restated, the STO layers grew in an islandlike manner such that a continuous film will form only when deposited for a sufficiently long interval. The film-to-substrate interaction can then be suppressed, and the formation of the perovskite PLZTO (PLTO) phase can thus be enhanced.

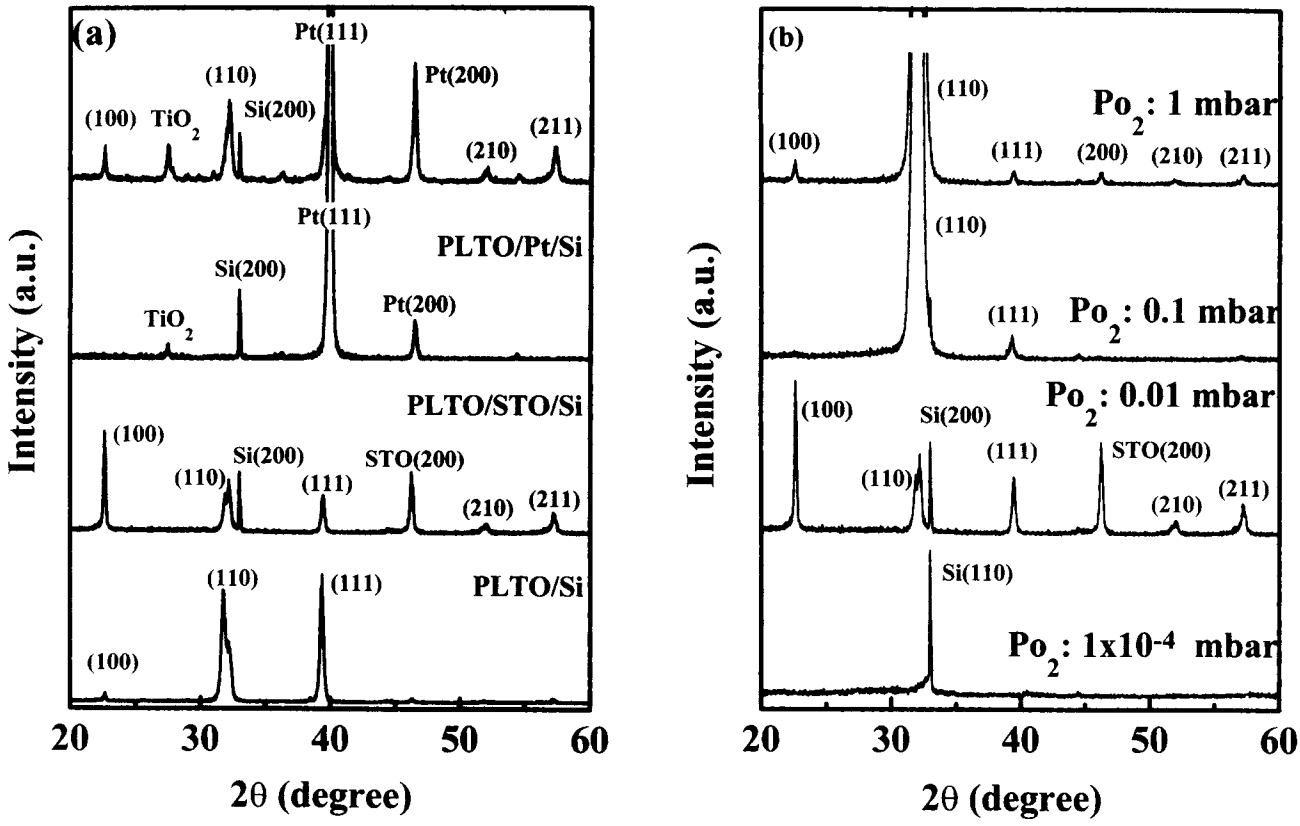

Figure 2. X-ray diffraction patterns of $Pb_{0.95}La_{0.05}TiO_3$ thin films deposited on: (a) STO-coated or uncoated Pt/Si (or Si) substrate (500°C, 1 mbar); (b) STO/Si substrates at 500°C under 1-, 0.1-, 0.01- and 1×10^{-4}-mbar oxygen pressure.

Bombardment damage

In order to understand what hinders the crystallization process of the films when the deposition oxygen pressure is low, the depth profile of the structure and the composition of PLTO thin films deposited on STO-coated Si substrates under $1\sim1\times10^{-4}$-mbar oxygen pressure were examined. The "phase" depth profiles for PLTO/STO/Si thin films shown as GIXD patterns in Figure 5a and 5b indicated that, when deposited under 1 mbar and 0.1 mbar oxygen pressure (500°C), only pure perovskite existed through the films. That is, no secondary phase occurred. The corresponding elemental depth profiles are represented by SIMS patterns in Figure 6a, which reveal that the ^{208}Pb and ^{47}Ti ion profiles are flat throughout the films. In other words, crystal structure and chemical composition are uniform throughout the films. No secondary phases or Pb deficiency are observed.

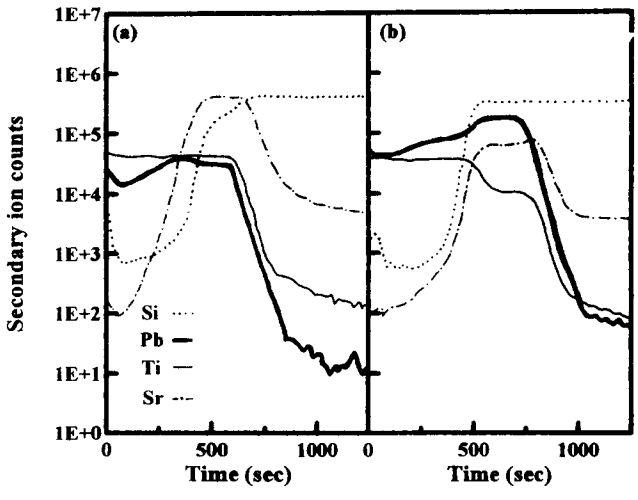

Figure 3. SIMS profiles of PLZTO thin films grown on Si substrate using (a) thick STO layer and (b) thin STO layer, which was deposited for 15 and 1 min, respectively, as precoatings.

However, the structure of the PLTO/STO/Si films is not as perfect when the deposition oxygen pressure was further decreased. The GIXD patterns corresponding to the films deposited under 1×10^{-2} mbar (500°C), as shown in Figure 5c, indicate that the crystalline phase can be detected for only $\theta > 1.0°$, and a broad hump was observed. These results infer that the outermost layer is amorphous and that the layer located underneath this amorphous layer is crystalline. The amorphorization of the deposited films is even more prominent when the deposition oxygen pressure is lowered further to 1×10^{-4} mbar (500°C). As shown in Figure 5d, only a broad hump was detected at $2\theta \approx 29°$. The elemental profiles of these films represented by the SIMS profile in Figure 6b, however, show that no appreciable Pb loss was observed, even in such a severe environment, which is inferred by the constant Pb-to-Ti ion count ratio throughout the thickness of the film. Hindrance of the crystallization process for adhered

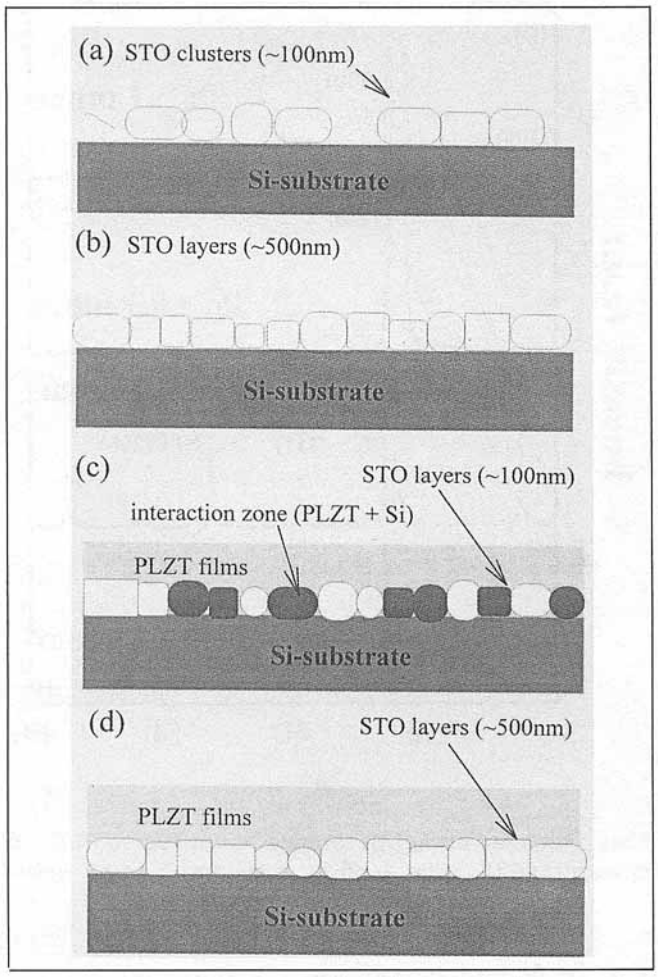

Figure 4. Thin-film growth sequence for deposition of STO and subsequent PLZTO thin films.

species is apparently not induced by the Pb deficiency in the films.

To facilitate the comparison of the interdiffusional behavior of the species, the reduction factors (RDFs), which were defined as the ratio of ion counts in the diffused layer to that in the original layer, of the ^{28}Si and ^{208}Pb species in the three layers were calculated from the SIMS profiles and listed in the third and fourth columns of Table 1. The RDFs of ^{28}Si in PLTO and that of ^{208}Pb in Si are small in PLTO/STO/Si films (Table 1, line (a)), showing that the interdiffusion of the ^{28}Si and ^{208}Pb ions between the PLTO and the Si layers has been substantially suppressed in the presence of the STO buffer layer. In contract, the RDF of the ^{28}Si in the STO is large for these films, revealing that the outward diffusion of the ^{28}Si ions from the Si to the STO layers is marked (Table 1, line (b)). Meanwhile, inward diffusion of ^{208}Pb and the ions from the PLTO to the STO layers is also pronounced, as indicated by the large RDF values of ^{208}Pb in STO (Table 1, line (c)). This is presumably the result of the high solubility of the Si and Pb species in STO materials.

The preceding analyses indicated that outward diffusion of ^{28}Si into the PLTO layer was insignificant and could not be the mechanism that induced the formation of amorphous PLTO films under low oxygen pressure. The other possible cause is the plume-to-film interaction, since the PLTO films synthesized by the PLD process were known to form by the transformation of the adhered species from the amorphous into the perovskite phase. To examine such a possibility, the characteristics of the laser-induced plume should be reviewed. It was proposed from the optical emission spectroscopic (OES) studies of Cheng (1995) that the plasma temperature (T_p) of the species in the laser-induced plume increased appreciably when the oxygen pressure (P_{O_2}) decreased below 0.01 mbar, that is, $T_p = 8{,}000$ K for $P_{O_2} = 1.0$ mbar or 0.1 mbar, and $T_p = 12{,}500$ K for $P_{O_2} = 0.01$ mbar and lower. The results shown in Figures 5a to 5d for the phase constituent of PLTO films deposited under 1 mbar to 1×10^{-4} mbar oxygen pressure indicated that the PLTO films are crystalline when the T_p value is low, and are amorphous when the T_p value is high. In other words, a noncrystalline phase was induced when the kinetic energy of the species in the plume was large.

Based on these observations, it is assumed that the formation of an amorphous phase under a low P_{O_2} environment is induced when the adhered clusters are subjected to the bombardment of the species with large kinetic energy. Such an interaction hindered the crystallization process. The lower the oxygen pressure was, the higher the kinetic energy of the incident species (Chrisey and Hubler, 1994), and the deeper the layer they damaged. The 1×10^{-4}-mbar-deposited PLTO films are therefore completely amorphorized, whereas the 1×10^{-2}-mbar-deposited ones are only partially amorphorized. In contrast, when $P_{O_2} = 1.0$ mbar or 0.1 mbar, the kinetic energy of the species is only low enough to enhance the mobility of adatoms that facilitate the crystallization of the adhered amorphous films. Obtained films are therefore fully crystallized.

Double-layer electrodes

A serious problem remained in using STO as a buffer layer for enhancing the crystallization kinetics of PLZTO and PLTO thin films. The STO buffer layer markedly degraded the PLZTO and PLTO ferroelectric properties due to its insulating nature. An approach to amend this kind of discrepancy is to utilize a conducting material as an intermediate layer, which not only enhances the formation of the PLZTO and PLTO phases but also serves as bottom electrodes. The Pt material possesses an overwhelming advantage in that it is stable, conducting and, best of all, is compatible with the device integration processes. It is interesting to observe that the perovskite PLTO structure formed at a lower substrate temperature on Pt-coated silicon substrates than that on uncoated silicon substrates (Yeh, 1995). The actual cause that enhanced the phase-transformation kinetics was investigated using SIMS and GIXD techniques. The GIXD patterns shown in Figure 7 for PLTO/Pt/Ti/Si films indicate that the PLTO phase already exists for $\theta = 0.1°$, and the intensity of PLTO peaks increased with the incident angle (θ). The GIXD patterns for the low incident angle corresponds to the X-rays diffracted from the outermost shallow layer of the films. The penetration of the X-ray beams increases with the θ value, and the diffraction peaks corresponding to larger θ value are provided by the thicker layer of the materials. Therefore, the GIXD patterns shown in Figure 7 represented the depth pro-

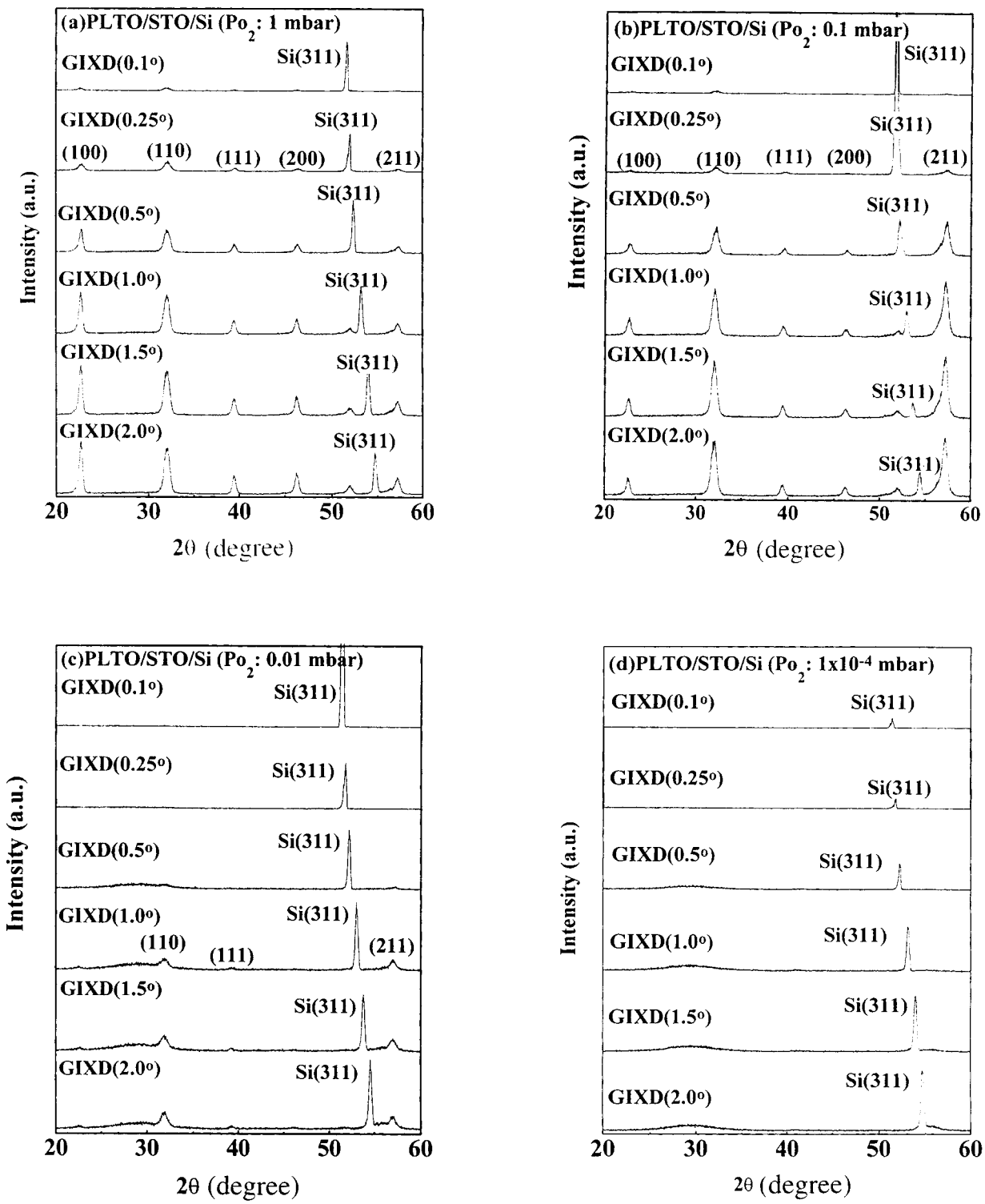

Figure 5. GIXD patterns of PLTO/STO/Si thin films deposited under (a) 1-, (b) 0.1-, (c) 0.01- and (d) 1×10^{-4}-mbar oxygen pressure.

file of the "phase" through the films. The increase in PLTO peaks with the θ value implied that the PLTO perovskite phase existed through the thickness of the films. The invariance in intensity of the TiO_2 peaks with the θ value indicated that the TiO_2 phase is a thin layer located somewhere in the multilayer thin films.

To further understand the structure of these multilayer thin films, the elemental depth profile of the PLTO/Pt/Ti/Si films was examined by SIMS, as shown in Figure 8a. The interdiffusion between layers was completely suppressed by the presence of the STO and Pt intermediate layers, as indicated by the rapid decrease in ^{28}Si and ^{208}Pb ion counts across the

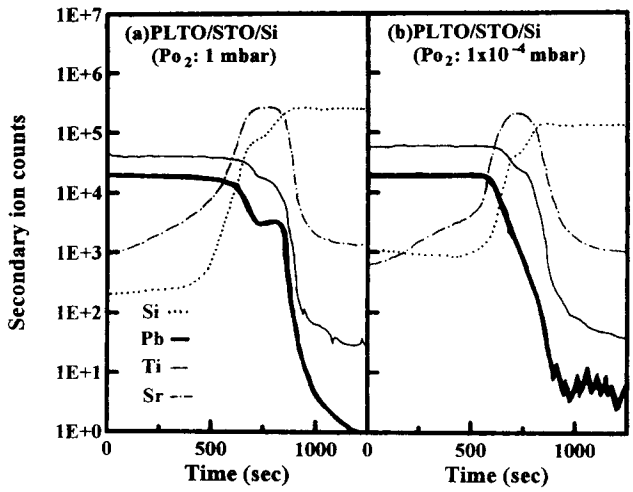

Figure 6. SIMS of PLTO thin films deposited on STO/Si substrates at 500°C under (a) 1-mbar and (b) 1×10^{-4}-mbar oxygen pressure.

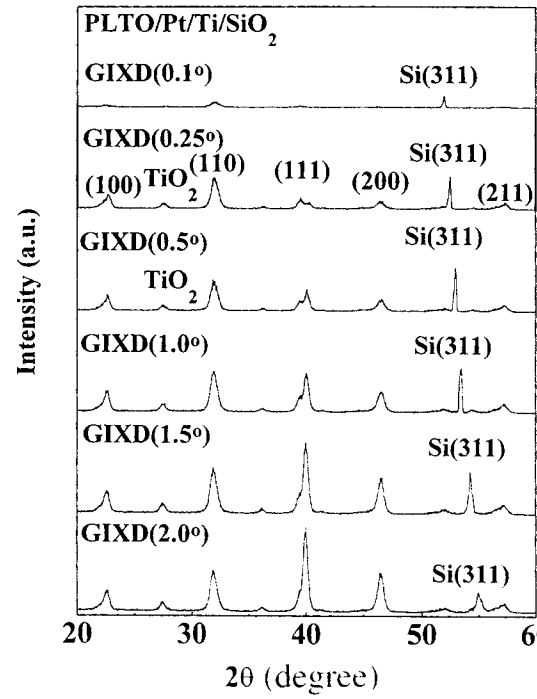

Figure 7. GIXD patterns PLTO/Pt/Ti/Si thin films.

intermediate layers. What should be noted is that there are two humps in the ^{47}Ti ion profile (labeled A and B) that occur beneath the PLTO layer. Hill A is apparently caused by the Ti films precoated on the Si substrate to improve the adhesion of the Pt-coatings. The occurrence of hill B is unexpected. It cannot be the Ti residue due to Pb-loss, since the SIMS patterns show that there is no Pb deficiency in the PLTO layers. It can only be accounted for by the outward diffusion of species in the Ti-precoating through the Pt-layer during the thin-film deposition process. It is therefore concluded from these results that the TiO_2 phase observed in the PLTO/Pt/Ti/Si thin films is a layer formed underneath PLTO due to outward diffusion of the underlying Ti-layer rather than Pb loss at the surface. The phenomenon of Ti-outward diffusion was also observed when the STO layer was precoated on top of the Pt layer to enhance the nucleation of the perovskite phase, shown as XRD patterns in Figure 2a and SIMS patterns in Figure 8b for the PLTO/STO/Pt/Ti/Si thin films with the RDFs' values listed in the fifth column of Table 1. Small RDFs of ^{28}Si in STO for the PLTO/STO/Pt/Si films indicate that the Pt layer can also clearly reduce the interdiffusion between the layers.

However, the PLTO/Pt/Ti/Si films are not stable enough to survive the high-temperature processing, as shown in Figure 9a, that where the perovskite phase is completely deteriorated for a substrate temperature higher than 650°C. Fortunately, the stability of the PLTO films can be substantially improved by using $(La_{0.5}Sr_{0.5})CoO_3$ (LSCO) as the intermediate layer. The PLTO/LSCO/Pt/Ti/Si films thus obtained can survive 650°C, as illustrated in Figure 9b. Interestingly, the SIMS profiles in Figure 8c show that the Ti species is still outward diffused through the Pt layer. Moreover, the preferred orientation of the PLTO films subsequently deposited on the LSCO layer inherited the texture characteristics of the underlying LSCO layer, namely, the [110] perferentially oriented PLTO thin films were deposited on [110] textured LSCO layer. The ferroelectric properties of PLTO films were optimized when deposited on LSCO/Pt, that is, with remanent polarization (Pr) around 14 ~ 16 $\mu C/cm^2$, coercive force (Ec) around 50 ~ 60 kV/cm, and relative dielectric constant (ϵ_r) around 900 ~ 1,000. The LSCO/Pt served as double-layer electrodes, in which the LSCO layer can facilitate the nucleation of the PLTO films, while the Pt layer provides an electrical conduction path.

Summary

Systematic studies of the various characteristics of $Pb_{1-x}La_x(Zr_yTi_{1-y})O_3$ (PLZTO) ferroelectric thin films with deposition parameters were reported. Elemental depth pro-

Table 1. Reduction Factor* of ^{28}Si and ^{208}Pb Species in the Multilayer Thin Films

Thin-Film Deposition Oxygen Pressure		PLTO/STO/Si 1 mbar	PLTO/STO/Si 1×10^{-4} mbar	PLTO/STO/Pt/Si 1 mbar
(a) PLTO-and-Si	^{28}Si in PLTO	1.0×10^{-3}	1.0×10^{-3}	0.3×10^{-3}
	^{208}Pb in Si	5.0×10^{-5}	3.0×10^{-5}	0.1×10^{-5}
(b) Si-to-STO	^{28}Si in STO	0.3**	0.3**	1.0×10^{-3}
(c) PLTO-to-STO	^{208}Pb in STO	0.15**	0.067**	0.01*

*RDF = ion counts to which species diffused/ion counts of original layer.
**Moderate interdiffusion.

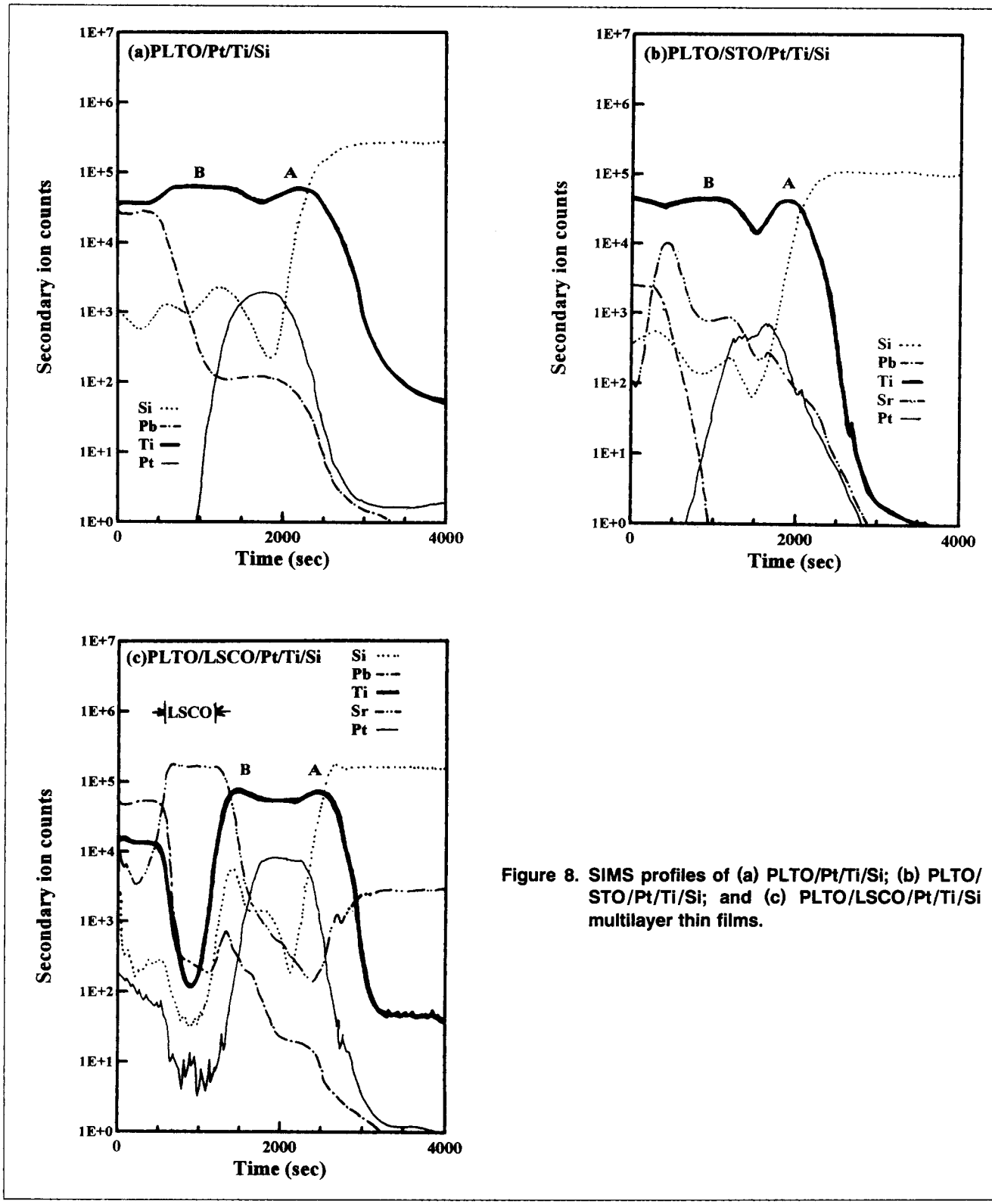

Figure 8. SIMS profiles of (a) PLTO/Pt/Ti/Si; (b) PLTO/STO/Pt/Ti/Si; and (c) PLTO/LSCO/Pt/Ti/Si multilayer thin films.

files examined by secondary-ion mass spectroscopy (SIMS), and structural profiles examined by grazing-incident X-ray diffraction (GIXD) were used to analyze the growth behavior of the thin films deposited by pulsed-laser deposition. Besides the high substrate temperature required, the chamber's oxygen pressure also substantially influenced the structure of the films. Oxygen pressure above $P_{O_2} = 1$ mbar resulted in insufficiently crystallized films, while $P_{O_2} < 0.01$ mbar led to the presence of an amorphous phase, which can be induced by bombarding the energetic species.

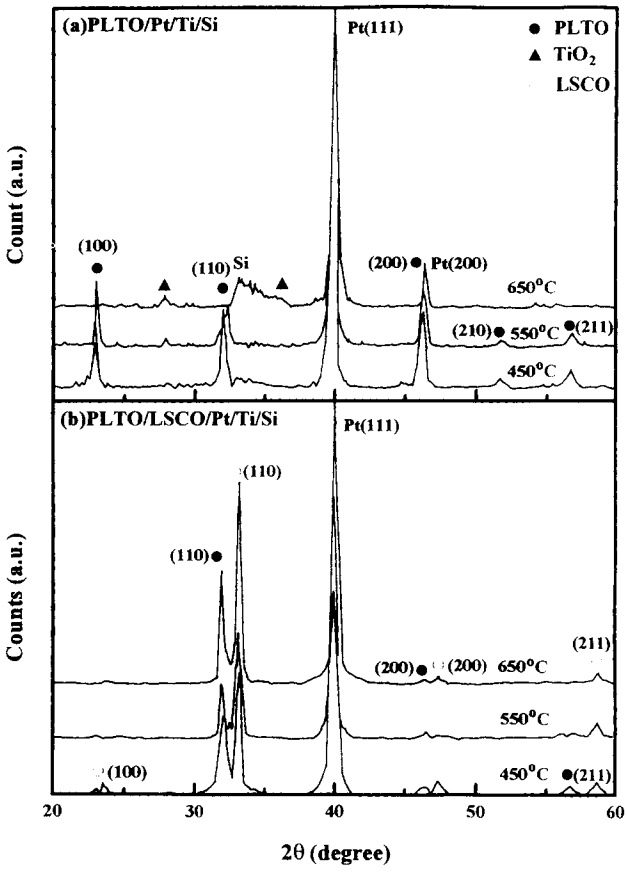

Figure 9. X-ray diffraction patterns of PLTO thin films deposited on (a) Pt/Ti/Si and (b) LSCO/Pt/Ti/Si substrates.

The presence of an intermediate layer modified the growth behavior by enhancing the nucleation of the crystalline phase during phase transformation. The proper choice of an intermediate layer, such as LSCO/Pt, not only prevented possible film-to-substrate interaction and Pb loss, but also led to preferentially oriented thin films and improved electrical properties.

Acknowledgments

Financial support by the National Science Council of the Republic of China through the Contract No. NSC 86-2112-M-007-032 is gratefully acknowledged by the authors.

Literature Cited

Cheng, H. F., "Spectroscopic Characteristics of $Pb_{0.95}La_{0.05}(Zr_{1-y}Ti_y)_{0.9875}O_3$ Plasma and Growth-Behavior of Thin Films by Pulsed Laser Deposition," *J. Appl. Phys.*, **78**, 4633 (1995).

Chrisey, D. B., and G. K. Hubler, *Pulsed Laser Deposition of Thin Films*, Wiley, New York (1994).

Gnadinger, F. P., and D. W. Bondurant, "Ferroelectrics for Nonvolatile RAMs," *IEEE Spectrum*, **7**, 30 (1989).

Grabowski, K. S., J. S. Horwitz, and D. B. Chrisey, "Pulsed Laser Deposition of Oriented $PbZr_{0.54}T_{0.46}O_3$," *Ferroelectrics*, **116**, 19 (1991).

Horwitz, J. S., K. S. Grabowski, D. B. Chrisey, and R. E. Leuchtner, "In Situ Deposition of Epitaxial $PbZr_xTi_{1-x}O_3$ Thin Films," *Appl. Phys. Lett.*, **59**, 2354 (1991).

Kidoh, H., T. Ogawa, A. Morimoto, and T. Shimizu, "Ferroelectric Properties of Lead-Zirconate-Titanate Films Prepared by Laser Ablation," *Appl. Phys. Lett.*, **58**, 2910 (1991).

Leuchtner, R. E., K. S. Grabowski, D. B. Chrisely, and J. S. Horwitz, "Anion-assisted Pulsed Laser Deposition of Lead Zirconate Titanate Films," *Appl. Phys. Lett.*, **60**, 1193 (1992).

Otsubo, S., T. Maeda, T. Minamikawa, Y. Yonezawa, A. Morimoto, and T. Shimizu, "Preparation of $Pb(Zn_{0.52}Ti_{0.48})O_3$ Films by Laser Ablation," *Jpn. J. Appl. Phys.*, **29**, 133 (1990).

Roy, D., S. B. Krupanidhi, and J. P. Dougherty, "Excimer Laser Ablated Lead Zirconate Titanate Thin Films," *J. Appl. Phys.*, **69**, 7930 (1991).

Scott, J. F., and C. A. P. de Araujo, "Ferroelectric Memory," *Science*, **246**, 1400 (1989).

Sheppard, L. M., "Advances in Processing of Ferroelectric Thin Films," *Ceram. Bull.*, **71**, 85 (1992).

Yeh, M. H., K. S. Liu, and I. N. Lin, "Formation of the Secondary Phases in the Pb-containing Perovskite Films by Pulsed Laser Deposition," *J. Mater. Res.*, **9**, 2379 (1994).

Yeh, M. H., K. S. Liu, J. P. Wang, Y. C. Ling, and I. N. Lin, "The Growth-Behavior of $Pb_{0.95}La_{0.05}(Zr_{1-y}Ti_y)_{0.9875}O_3$ Films on Silicon Substrates Synthesized by Pulsed Laser Deposition," *J. Appl. Phys.*, **77**, 5335 (1995).

Manuscript received Oct. 28, 1996, and revision received July 21, 1997.